The Emerald Research Register for this journal is available at
http://www.emeraldinsight.com/researchregister

The current issue and full text archive of this journal is available at
http://www.emeraldinsight.com/0961-5539.htm

Numerical model for vacuum infusion manufacturing of polymer composites

H. Magnus Andersson, T. Staffan Lundström and B. Rikard Gebart
Division of Fluid Mechanics, Luleå University of Technology, Sweden

Received November 2001
Revised October 2002
Accepted November 2002

Keywords *Porous media, Composite materials, Numerical methods*

Abstract *The focus is set on the development and evaluation of a numerical mgodel describing the impregnation stage of a method to manufacture fibre reinforced polymer composites, namely the vacuum infusion process. Examples of items made with this process are hulls to sailing yachts and containers for the transportation industry. The impregnation is characterised by a full 3D flow in a porous medium having an anisotropic, spatial- and time-dependent permeability. The numerical model has been implemented in a general and commercial computational fluid dynamic software through custom written subroutines that: couple the flow equations to the equations describing the stiffness of the fibre reinforcement; modify the momentum equations to account for the porous medium flow; remesh the computational domain in each time step to account for the deformation by pressure change. The verification of the code showed excellent agreement with analytical solutions and very good agreement with experiments. The numerical model can easily be extended to more complex geometry and to other constitutive equations for the permeability and the compressibility of the reinforcement.*

Introduction

There are numerous ways to manufacture fibre reinforced polymer composites ranging from hand lay-up in small series to fully automatic pressing of components to the automotive industry. A method that is being increasingly used for production in small series is the vacuum infusion process. The advantage with this method is that large and high strength items can be produced in relatively low cost tooling and with low emissions of harmful substances. Examples of products are hulls to sailing yachts and containers for the transportation industry. The vacuum infusion technique is well known and established since long. The first patents are registered already in 1950 (Marco method, 1950). Still, process development has until recent years mainly been based on trial and error and the behaviour of the process is therefore not fully understood and the modelling is so far not sufficient (Smith, 1999; Williams *et al.*, 1996). The risk of severe economic losses in the case of an unsuccessful

This work was supported by the Swedish Research Council for Engineering Sciences (TFR). We are happy to acknowledge the contributions from Anna-Maria Gustafsson, Henrik Jacobsson and Olle Törnblom at Luleå University of Technology who performed the early work on the numerical model.

International Journal of Numerical Methods for Heat & Fluid Flow
Vol. 13 No. 3, 2003
pp. 383-394

0961-5539
DOI 10.1108/09615530310464553

charge is augmented with an increased part size and the corresponding increase in material value. An essential requirement for an optimised and reliable processing is therefore the development of tools that can guide the processing engineers in the choice of reinforcement, flow enhancing technique, injection strategy, injection parameters, etc.

The fundamental principle of the vacuum infusion process is that dry fibre reinforcement is placed on a stiff mould half and covered with a flexible and airtight bag. The bag is then sealed to the mould except at certain positions being open for resin supplies and outlets. By keeping atmospheric pressure at the resin inlets and reducing the pressure at one or several positions in the formed cavity, liquid resin is forced to impregnate the reinforcement. A further result of the difference between the ambient pressure and the pressure within the cavity is a compaction force and a corresponding compression of the elastic stack. Once the mould is sufficiently filled, the pressure in the cavity is evened out and the resin is cured. In order to shorten the cycle-time, flow enhancing methods are often used with the vacuum infusion process. This may result in an important out-of-plane flow at the flow-front that is often neglected in the modelling of the well-characterised process resin transfer moulding (RTM). Another difference from RTM is the variation of height of the cavity as a function of the local pressure, implying that the flow and compaction equations become coupled.

To increase the understanding of the vacuum infusion process we have performed a study of real mouldings in a simple geometry (Andersson *et al.*, 2002, 2003). In particular, a Digital Speckle Photography system has been used to measure the overall movement of the reinforcement and the through thickness flow-front has been measured with flow visualisation, video recording and image analysis. The experimental study was confined to one geometry and one particular material combination. A generalisation of the results to form prevalent conclusions and rules-of-thumb is therefore inevitable. One step towards a generalisation was presented by Hammami and Gebart (1998) where a 1D model was derived. In this paper, we move further by performing simulations on the vacuum infusion process in a general 3D computational fluid dynamics (CFD) code. The advantage of taking such an approach is that the calculations are based on equations tested in numerous applications, that we can do simulation in almost any geometry, and that we, quite easily, can extend our simulations to deal with other constitutive equations and additional phenomena.

Analytical background

During all fabrication of fibre reinforced composites the resin is, in some way, forced into the fibre network. In order to predict the time for the resin to fill a certain volume of pore space between fibres and the corresponding filling pattern, analytical expressions and mould filling simulation codes have been developed (Diallo *et al.*, 1998; Fracchia and Tucker III, 1990; Gebart *et al.*, 1992;

Koorevar, 1995). These tools are mainly designed for the RTM process with stiff moulds and are based on conservation of mass and Darcy's law which in 2D may be expressed as:

$$u_{i,i} = 0 \tag{1a}$$

$$u_i(1-f) = -\frac{K_{ij}}{\mu} p_j \quad i,j = 1,2 \tag{1b}$$

where u is the volumetric flux density (also called superficial velocity) in the fibre preform, f is the fibre volume fraction, K is the permeability of the fibre preform, μ is the viscosity of the resin and p is the pressure. The combination of equation (1(a) and (b)) applies to flow in the porous media as long as the Reynolds number is sufficiently low, the fibres are stationary and the fluid is incompressible and can be modelled as Newtonian. In the vacuum infusion process the fibres are allowed to move in the through thickness direction and the equations are modified accordingly (Hammami and Gebart, 1998):

$$(uh)_{i,i} = -\frac{\partial h}{\partial t}, \tag{2a}$$

$$p + p_{\mathrm{r}} = p_0, \tag{2b}$$

$$K_{ij} = g^1_{ij}(h), \tag{2c}$$

$$h = g^2(p_{\mathrm{r}}) \tag{2d}$$

where h is the height of the stack, p_{r} is the pressure on the reinforcement, p_0 is the ambient pressure and $g^{1,2}$ are the constitutive functions. These functions can be derived experimentally from permeability and compaction measurements. Fortunately, only a few measurements are required since a number of theoretical models have been proposed. Two models for the permeability were presented by Gebart (1992) for flow along and perpendicular to a perfect arrangement of fibres. Both these models are expressed in terms of the fibre volume fraction, f and the fibre radius R according to:

$$K_{\parallel} = \frac{8}{c}\frac{(1-f)^3}{f^2}R^2, \tag{3a}$$

$$K_{\perp} = C\left(\sqrt{\frac{f_{\max}}{f}} - 1\right)^{5/2} R^2, \tag{3b}$$

$$f = \frac{n\zeta}{h\rho_s} \tag{3c}$$

The maximum fibre volume fraction $f_{\max}$ and the two constants c and C are dependent on the actual fibre arrangements, e.g. quadratic or hexagonal packing, n is the number of layers of the fabric, ζ is the weight per unit area of each fabric layer and ρ_s is the density of the fibres. The first of these equations is based on the hydraulic radius and can be recognised as the often-used Kozeny-Carman equation. The relation between the pressure on the reinforcement and the height of it is often written in the following form (Toll, 1998):

$$p_{\mathrm{r}} = kE(f^m - f_0^m) \tag{4}$$

where k and m are constants, E is the stiffness of the fibres and f_0 is the fibre volume fraction of the reinforcement without any load. By a micromechanical analysis it has been shown that the constant m is equal to 3 for 3D wads and 5 for planar networks (Toll, 1998). Many reinforcements used in vacuum infusion do, however, consist of continuous fibre bundles. For such materials m has empirically been given values spanning from 7 to 16 (Lundström and Sandlund, 1997; Toll, 1998). It has been further shown that the stiffness is reduced by lubrication of the fibres when the reinforcement is impregnated with resin (Andersson *et al.*, 2002, 2003; Toll, 1998; Williams *et al.*, 1998). To be able to account for the new elastic response in the numerical model, equation (4) must be adjusted. A true modification can be derived from compaction measurements of wetted and dry reinforcements. We will however, at this stage take a heuristic approach and use the following relationship:

$$p_{\mathrm{r}} = kE(f^m - (f_0 + \kappa)^m) \tag{5}$$

where κ accounts for the softening of the reinforcement and is consequently, zero for a dry fabric and larger than zero for a wetted fabric.

The equations required to model the impregnation taking place during vacuum infusion have now been outlined. These equations were previously solved in a quasi-stationary way with flow in one direction only (Hammami and Gebart, 1998). However, to get a complete solution another approach must be used. We will here present such an approach based on a general CFD-code.

Numerical model

A general application of the numerical solution method to a physical problem involves the choice of the mathematical model, discretisation method, coordinate system, numerical grid, iterative methods, etc. Here, the eligibility is defined to the components available in the commercial and general CFD software CFX-4 from AEA Technologies. CFX-4 is a finite-volume based code using a structured multi-block grid. The code offers a number of choices regarding, for instance, the mathematical models and iterative methods and it handles moving boundaries by the volume of fluid algorithm (Ferziger and Peric, 1999). The latter was naturally crucial in the choice of code while the former facilitate a development of the model to similar processes and other materials. The modelling of the vacuum infusion process in CFX implies several subtle challenges and we shall deal with these in due order.

Governing equations and the finite volume method

The equations to be solved are the general conservation laws. In Cartesian coordinates using tensor notation, the differential form of the full 3D generic conservation equation is (Ferziger and Peric, 1999):

$$\frac{\partial(\rho\phi)}{\partial t}+\frac{\partial(\rho v_j\phi)}{\partial x_j}=\frac{\partial}{\partial x_j}\left(\Gamma\frac{\partial\phi}{\partial x_j}\right)+q_\phi \tag{6}$$

where Γ is the diffusivity of the considered quantity ϕ, ρ is the density of the fluid and v_j is the actual fluid velocity (rather than the superficial velocity used in equation (1) and (2). For conservation of mass, where $\phi = 1$, equation (6) simply reduces to the continuity equation and for conservation of momentum, where $\phi = v_i$, it reduces to the Navier-Stokes equations for a Newtonian fluid. By changing the coefficients and adding source terms (q_ϕ), equation (6) can be modified to correspond to the applied conditions. Most commercial CFD-codes allow such modifications. The finite volume method solves the integral form of the generic conservation equation (equation (6)):

$$\frac{\partial}{\partial t}\int_\Omega \rho\phi\,\mathrm{d}\Omega+\int_S \rho\phi v_j n_j\,\mathrm{d}S=\int_S \Gamma\frac{\partial\phi}{\partial x_j}n_j\,\mathrm{d}S+\int_\Omega q_\phi\,\mathrm{d}\Omega \tag{7}$$

In fluid flow it is more convenient to deal with the flow within a certain spatial region rather than with a given quantity of matter. The solution domain is therefore, divided into a finite number of control volumes (CV), where Ω and S denote the volume and the surface of a CV and n_j its surface normal. Equation (7) is applied to each CV, ensuring conservation for both the single CV and the whole solution domain, i.e. the method is conservative by construction. Approximating surface and volume integrals by appropriate quadrature formulae results in an algebraic equation for each CV (Ferziger and Peric, 1999).

Flow through porous media

The geometry of the individual fibres in the reinforcement is in this case clearly too complex to be resolved with a grid. Instead, the Navier-Stokes equations are modified to account for the extra pressure drop in the flow generated by the flow through the porous medium. This is implemented while retaining both advection and diffusion terms (AEA Technology plc., 1999). The mathematical representations of the alteration are the transfer terms for the interaction between fluid and solid, in addition to the usual pressure gradient and diffusion terms in the momentum equation. With γ as the volume porosity scalar and A_{ij}

as the area porosity tensor for a porous medium, the general scalar equation (equation (6)) for the conservation of momentum for an incompressible fluid is:

$$\frac{\partial}{\partial t}(\gamma\rho v_i) + (\rho A_{jk} v_k v_i)_j - \mu(A_{jk}(v_{k,i} + v_{i,k}))_j = -\gamma R_{ji} v_i - \gamma p_j \tag{8}$$

where R_{ij} represents a resistance to the flow in the porous medium, proportional to the inverse of the permeability, K_{ij}^{-1}. Equation (8) corresponds to Brinkman's equation (Kaviany, 1995). If the permeability is low, the first term on the right hand side of equation (8) becomes large and is balanced by the pressure gradient term, while the advective and viscous terms on the left hand side are negligible in comparison. Thus, in the limit of a large resistance and stationary flow, equation (8) reduces to:

$$0 = R_{ji} v_i + p_j \tag{9}$$

which is identical to Darcy's law (equation (1(a))). Hence, the final outcome of importance here is that in CFX-4, where equation (8) is solved, the results will be the same as if Darcy's law (equation (1(a))), was solved.

Moving boundaries

We will encounter two types of moving boundaries. First, the impregnation process is modelled as homogeneous two-phase flow with a free surface. Mathematically this implies that the momentum equations yield identical velocity fields for both phases, except for the volume fractions, which are obtained by solving separate continuity equations. This approximation is valid since the volume fractions are close to either zero or unity in the majority of the control volumes. An appropriate initial specification of the volume fractions of the two phases is a sharp change across the interface separating them. Due to numerical diffusion, the interface will become geometrically smeared out with time. In order to conserve the initial sharpness of the interface, CFX-4 provides a special surface sharpening algorithm for two-phase flows (AEA Technology plc., 1999). Provided the mesh is fine enough to resolve the free surface, the algorithm identifies fluid on the wrong side of the interface and moves it to the correct side, with the condition that volume is at all times conserved. Also, each time step should allow the flow-front to advance not more than one computing cell at a time.

Second, the deformation of the reinforcement due to the combination of external pressure and internal pressure in the form of resin pressure and reinforcement stiffness defines the other type of moving boundary. The thickness of the stack is calculated based on a force balance according to equation (5), where the difference between wet and dry reinforcement has been included. The permeability is then updated according to equation (3(a)). This is followed by iterations of the solution for a new pressure distribution. When convergence is achieved, a new time step is applied and the whole procedure is repeated from the beginning. At all times, the numeric grid has to be updated to the changes in geometry.

Verification and validation of model with stiff mould

Verification is defined by Roache (1998) as a demonstration that the numerical solution of a set of partial differential equations is correct, while *validation* is defined as a demonstration that the chosen set of equations is the best possible representation of the real physical situation. We shall start the verification process by solving Darcy's law for a transient flow through a porous medium between the parallel solid boundaries. The analytical solution for an isotropic permeability is (Gebart, 1992):

$$x_{\mathrm{f}}^2 = \frac{2K\Delta p}{\mu(1-f)}\,t \tag{10}$$

where x_{f} is the flow-front position measured from the inlet and t is time. In order to compare the results from the numerical solution to the analytical solution, i.e. to verify the numerical model, both solutions are carried out for a real case (Andersson *et al.*, 2002, 2003). The permeability of the reinforcement is set to $9.2\times 10^{-11}\,\mathrm{m}^2$, the driving pressure to 0.1 MPa, the resin viscosity to 0.180 Pas and the fibre volume fraction to 52.5 per cent. The solid dots in Figure 1 represent the numerical solution, for which the smallest time steps are of order 10^{-2} s, whereas the straight line is predicted by equation (10). A straight line fitted to the numerical solution reveals a difference from the analytical solution of less than 1 per cent. Even though the error from truncation errors,

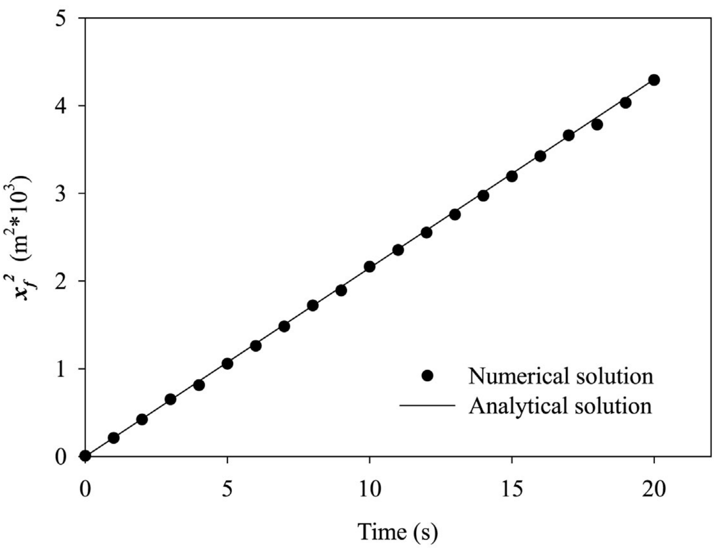

Figure 1. Numerical solution (dots) and analytical solution (straight line) for transient flow through a porous medium of isotropic permeability between parallel solid boundaries

etc., could probably be decreased further by grid refinement and tighter iterative convergence criterion, this error level was considered acceptable.

Now, bringing the verification process one step further, we study the more general case of two materials of equal thickness (10 mm), one on top of the other, each with a different and non-isotropic permeability. The curves in Figure 2 show the resulting flow-front at different time steps (1, 5 and 13 s, respectively) as calculated by the CFD-code whereas, the solid dots are predicted by a traditional RTM simulation program solving Darcy's law (Koorevaar, 1995). As an indirect verification, Figure 2 shows an excellent agreement. For reference, the ratio of the in-plane permeability and the through thickness permeability is 10 for both materials, which is also the ratio of the in-plane permeability for the two materials as compared to each other.

For the validation process we turn to experimental result presented by Gebart *et al.* (1991). Again, we study the general case of two materials of equal thickness, s, one on top of the other. Now we let both the materials to have different but isotropic permeability, K_1 and K_2, meaning that the permeability in the through thickness direction and in the in-plane direction is equal within each material. Also, the fibre volume fraction is assumed to be the same for both materials. Under these conditions, it has been shown both analytically and experimentally (Gebart *et al.*, 1991; Fracchia and Tucker III, 1990) that the ratio of the flow-front lead-lag l (Sun *et al.*, 1998) and the layer thickness s is a linear function of $\sqrt{K_1/K_2}$ with an experimentally obtained constant of proportionality of 0.38. The solid straight line in Figure 3 with a slope of 0.37 is a best fit to numerical solutions (solid dots) obtained with the CFD-code for the shown permeability ratios and a fibre volume fraction of 50 per cent. Thus, the overall conclusion is that the new CFD-based model is an acceptable approximation of the mathematical model for vacuum infusion.

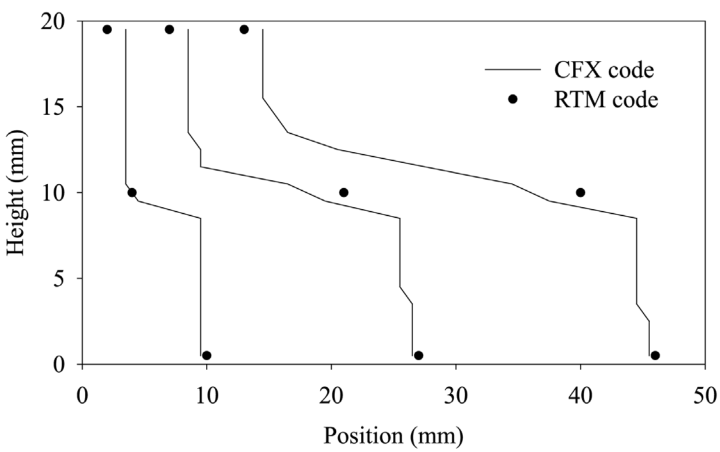

Source: Koorevaar (1995)

Figure 2.
Numerical solutions for transient flow through two non-isotropic materials of equal height between solid parallel boundaries. With flow from left to right, the curves represent the flow-front after 1, 5 and 13 s, respectively. The solid dots are solutions obtained with an RTM-code

Examples of simulations with the full model

We will here exemplify the strength of the developed method by results from three simulations in a simple geometry. The results are illustrated by the liquid volume fraction in the pores during the injection and the corresponding pressure distribution in the resin. First, consider a low Reynolds number and parallel flow of a Newtonian liquid into a porous medium having a constant permeability. With the medium confined in a mould consisting of two parallel and stiff plates, the pressure gradient is constant. This is exemplified in Figure 4 where uniformly distributed isobars are presented as the vertical lines.

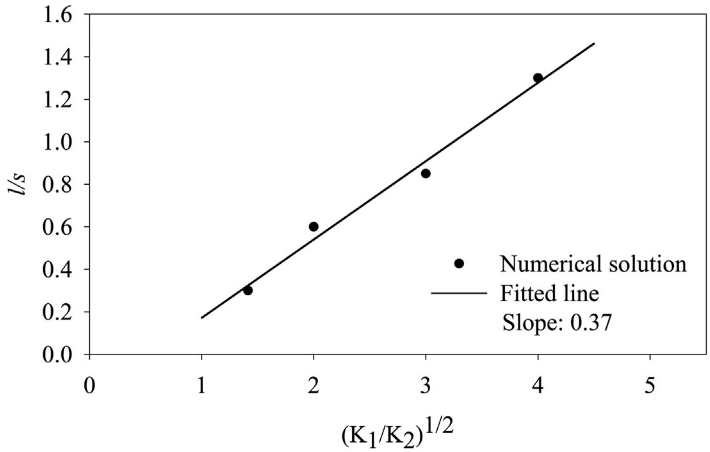

Note:
The straight line represents the analytical solution and the solid dots are numerical solutions

Figure 3.
Scaled flow-front lead-lag versus the square root of the permeability ratio for flow through two isotropic materials of equal height between solid parallel boundaries

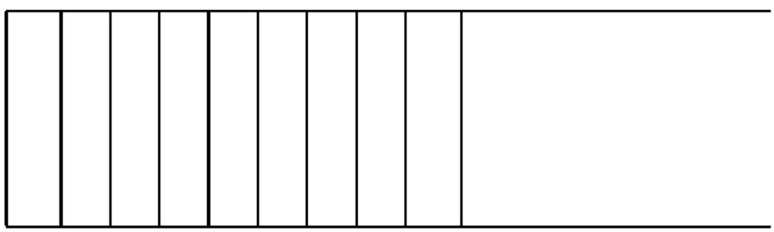

Note:
The highest pressure is at the inlet to the left. The regular position of the isobars indicates a constant pressure gradient in the flow direction

Figure 4.
Evenly distributed isobars (the vertical lines) as obtained with the CFD-code for parallel flow of a Newtonian liquid into a porous medium with constant and isotropic permeability placed between two parallel stiff plates

However, the pressure distribution changes in accordance with the shape of the flow-front when two layers of fibre reinforcement with different permeability are used, cf. Figure 5. Here the ratio of the in-plane permeability of the upper layer, K_1, and the in-plane permeability of the lower layer, K_2, is 10. The permeability in the transverse direction is held constant and equal to K_2 in both layers.

In the last example, shown in Figure 6, the upper stiff mould is replaced by a flexible bag, cf. equation (5) with $\kappa = 0.1$, $kE = 289.5 \times 10^{-6}$, $f_0 = 0.42$ and $m = 14.19$. Now the thickness of the stack is largest at the inlet where the pressure in the resin approaches the ambient pressure. Moving towards the outlet where the vacuum level is highest, the thickness becomes smaller and smaller. Also, the decrease in stiffness as a result of lubrication of the fibres results in a thickness and consequently the permeability is minimum at the flow-front.

As can be confirmed by a qualitative comparison between Figures 4 and 6, these effects result in a small but detectable difference in pressure distribution. It should be noticed that the value of κ that is employed has simply been

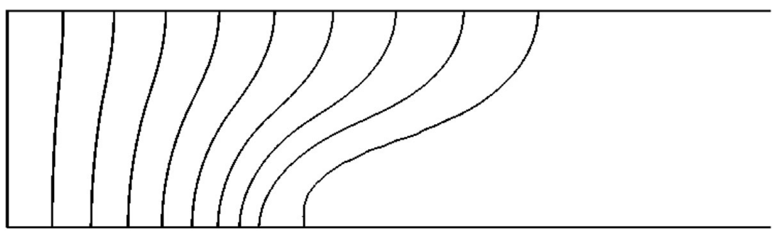

Figure 5.
Evenly distributed isobars as obtained with the CFD-code for flow of Newtonian liquid in two layers of fibre reinforcement with different permeability

Note:
The highest pressure is at the inlet to the left

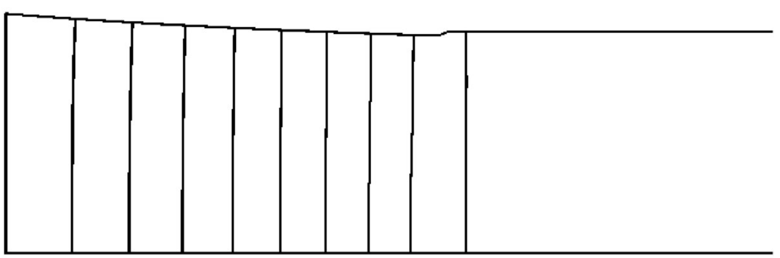

Figure 6.
Evenly distributed isobars as obtained with the CFD-code when the upper boundary is a flexible bag

Note:
The highest pressure is at the inlet to the left. The thickness of the stack decreases towards the outlet but because of a change in stiffness due to wetting of the fibres a thickness minimum is observed instantly behind the resin flow-front

guessed and the other values used in Figure 6 are valid for one fabric only (Lundström and Sandlund, 1997). To what extent alterations of these quantities will influence the impregnation process is the subject of ongoing work in our group.

Conclusions and future work

It has here been shown that the general and commercial CFD-code CFX-4 can be used for simulations of the vacuum infusion process. As compared to standard RTM-simulation programs it is possible to account for the effects of through thickness flow. In contrast to RTM-codes the new model also accounts for thickness variations during impregnation, which is crucial for a realistic model (Andersson *et al.*, 2002, 2003). The verification of the code showed an excellent agreement to analytical expressions and excellent conformity with simulations done with an RTM-code. Validation of the model against impregnation of a heterogeneous stack of reinforcements indicates that the chosen set of equations is a most adequate representation of reality.

Future work will involve further validation of the code against experimental results (Andersson *et al.*, 2002, 2003) and simulation of vacuum infusion of real components. Furthermore, the code will be used to form general guidelines for the vacuum infusion process. Finally, we will investigate the possibility of process optimisation and studies of the effect of new types of materials and processing conditions.

References

AEA Technology plc. (1999), "CFX 4.3: solver", CFX-International, Oxfordshire, UK.

Andersson, H.M., Lundström, T.S., Gebart, B.R. and Långström, R. (2002), "Flow enhancing layers in the vacuum infusion process", *Polymer Composites*, Vol. 23 No. 5.

Andersson, H.M., Lundström, T.S., Gebart, B.R. and Synnergren, P. (2003), *Polymer Composites*, Vol. 24 No. 3.

Diallo, M.L., Gauvin, R. and Trochu, F. (1998), "Experimental analysis and simulation of flow through multi-layer fiber reinforcements in liquid composite molding", *Polymer Composites*, Vol. 19 No. 3, pp. 246-56.

Fracchia, C.A. and Tucker III, C.L. (1990), "Simulation of resin transfer mold filling", *6th Annual Meeting of the Polymer Processing Society*, Nice, France.

Ferziger, J.H. and Peric, M. (1999), *Computational Methods for Fluid Dynamics*, Springer, Berlin.

Gebart, B.R. (1992), "Permeability of unidirectional reinforcements for RTM", *Journal of Composite Materials*, Vol. 26 No. 8, pp. 1100-33.

Gebart, B.R., Gudmundson, P., Strömbeck, L.A. and Lundemo, C.Y. (1991), "Analysis of the permeability in RTM reinforcements", *8th International Conference on Composite Materials*, Honolulu, USA.

Gebart, B.R., Lundemo, C.Y. and Gudmundson, P. (1992), "An evaluation of alternative injection strategies in RTM", *47th Annual Conference of the Society of Plastics Institutes*, Cincinatti, USA.

Hammami, A. and Gebart, B.R. (1998), "Model for vacuum infusion moulding process", *Plastics, Rubber and Composite Processing and Applications*, Vol. 27 No. 4, pp. 185-9.

Kaviany, M. (1995), *Principles of Heat Transfer in Porous Media*, Springer, New York.

Koorevaar, A. (1995), "Simulation of the resin transfer moulding (RTM) process", *Techtextil-Symposium*.

Lundström, T.S. and Sandlund, E. (1997), "Permeability and compression of RTM reinforcements", in Bäcklund, J., Zenkert, D. and Åström, B.T. (Eds), *Composites and Sandwich Structures*, EMAS Publishing, Stockholm.

Marco method (1950), US Patent No. 2495640.

Roache, P.J. (1998), *Verification and Validation in Computational Science and Engineering*, Hermosa Publishers, Albuquerque.

Smith, F.C. (1999), "The current status of resin infusion as an enabling technology for toughened aerospace structures", *Materials Technology*, Vol. 14 No. 2, pp. 71-80.

Sun, X., Li, S. and Lee, L.J. (1998), "Mold filling analysis in vacuum-assisted resin transfer molding. Part 1: SCRIMP based on a high-permeable medium", *Polymer Composites*, Vol. 19 No. 6, pp. 807-17.

Toll, S. (1998), "Packing mechanisms of fiber reinforcements", *Polymer Engineering and Science*, Vol. 38 No. 8, pp. 1337-50.

Williams, C.D., Summerscales, J. and Grove, S.M. (1996), "Resin infusion under flexible tooling (RIFT): a review", *Composites Part A*, Vol. 27A, pp. 517-24.

Williams, C.D., Grove, S.M. and Summerscales, J. (1998), "The compression response of fibre-reinforced plastic plates during manufacture by the resin infusion under flexible tooling method", *Composites Part A*, Vol. 29A, pp. 111-14.